Copyright © 2013 Tech Science Press CMES, vol.94, no.6, pp.507-527, 2013

# ACA-accelerated Time Domain BEM for Dynamic Analysis of HTR-PM Nuclear Island Foundation

**Haitao Wang**[1,2], **Zhenhan Yao**[3]

**Abstract:** This paper presents the use of a three-dimensional time domain boundary element method (BEM) in conjunction with adaptive cross approximation method (ACA) for dynamic analyses of the HTR-PM nuclear island foundation. The advantage of this approach is that only foundation of the HTR-PM nuclear island and limited surfaces of the supporting half-space soil medium are modeled and analyzed in a direct time stepping scheme. In addition, the ACA can compress the BEM coefficient matrices at each time step efficiently, therefore allowing larger models to be analyzed compared with conventional BEMs. In order to discretize the boundary integral equation (BIE) we use collocation method and eight-node discontinuous quadratic element. In order to preserve the causality condition an element subdivision technique suggested by Marrero (Engineering Analysis with Boundary Elements 2003; 27: 39–48) is adopted. In the numerical tests, sensitivity analyses are carried out in order to study dynamic characteristics of the HTR-PM nuclear island foundation and to establish fixed base criteria of the supporting soil medium for the associated seismic design of the nuclear island.

**Keywords:** boundary element; time domain; adaptive cross approximation; HTR-PM; foundation

## 1 Introduction

Earthquake is one of the most severe issues affecting safety of the nuclear power plants (NPPs). In the seismic design of a NPP, it is required to evaluate the dynamic effect of nuclear island foundation-supporting soil interactions. When the shear wave velocity of the soil is high enough, it is acceptable to assume the soil as a

[1] Institute of Nuclear and New Energy Technology, Tsinghua University, Beijing 100084, P. R. China.
[2] Corresponding author.
Tel.: +86 10 6279 7882; fax: +86 10 6279 7136; Email: wanght@tsinghua.edu.cn
[3] School of Aerospace, Tsinghua University, Beijing 100084, P. R. China.
Email: demyzh@tsinghua.edu.cn

fixed base for the foundation. During the licensing process of a NPP design, such fixed base assumption commonly remains considerable discussions. Specifically, the high-temperature-reactor pebble-bed module (HTR-PM) [Zhang, Wu, Sun and Li (2006)], a Chinese design of the high temperature gas-cooled reactor (HTR), has three nuclear-grade buildings sharing one common foundation. It is of strong interest to study dynamic characteristics of such large, irregular foundation under various soil profiles and to set up a fixed base criterion for the following seismic design.

Much effort has been made with various numerical methods on the study of dynamic foundation-soil interactions. As a boundary-type numerical method, the boundary element method (BEM) is particularly suitable for modeling such half-space dynamic problem as only the foundation and limited surface of the soil need to be meshed. In addition, the radiation condition is automatically satisfied. For the boundary integral equation (BIE) formulations for elastodynamics, one can conduct Cruse and Rizzo (1968) in Laplace domain, Domı'nguez (1993) in Fourier domain and Mansur (1983) and Antes (1985) in direct time domain. Dynamic BEM analysis of strain gradient elastic problems was also reviewed [Tsinopoulos, Polyzos and Beskos (2012)]. Applications of the BEM for the foundation-soil interaction analyses have been continuously reported. For comprehensive reviews in this field, one can conduct Beskos (1987 and 1997). Compared with frequency domain BEMs, the time domain BEM provides a direct assessment of dynamics behaviors versus time. In order to improve its stability, various techniques have been introduced [Rizos and Karabalis (1994); Peirce and Siebrits (1997); Mansur and Carrer (1998); Yu, Mansur, Carrer and Gong (1998); Birgisson, Siebrits and Peirce (1999)]. In addition, the Convolution Quadrature method (CQM) [Lubich (1988, 2004)] has drawn more and more attentions due to its intrinsic stable feature and its ability to treat fundamental solutions in Laplace domain. The time domain BEM in conjunction with CQM has been employed for elastic, visco-elastic and poro-elastic dynamic problems [Schanz and Antes (1997); Gaul and Schanz (1999); Schanz (2001); Kielhorn and Schanz (2008)].

Conventionally, the coefficient matrix of the BEM is dense with $O\left(N^2\right)$ storage, where $N$ is the number of unknowns. Solving such BEM equation requires $O\left(N^2\right) \sim O\left(N^3\right)$ operations with direct or iterative algorithms. This becomes a bottleneck of the BEM, especially for elastodynamics where a large number of BEM matrices need to be stored. In order to achieve large-scale BEM solutions, several fast algorithms have been implemented in this field. Of particular interest are the fast multipole method (FMM) [Rokhlin (1985); Rokhlin and Greengard (1997)] and the adaptive cross approximation method (ACA) [Bebendorf (2003)]. The FMM is an $O(N)$ algorithm in both computational time and storage which requires suitable expansion formulations of the associated kernel functions. The ACA however, is a kernel-independent fast algorithm which requires only the knowledge of matrix entries. Fast BEM applications for elastostatics by using FMM [Fu, Klimkowski, Rodin and colleagues (1998); Helsing (1999); Popov and Power (2001); Yoshida, Nishimura and Kobayashi (2001); Liu, Nishimura, Otani and colleagues (2005); Wang and Yao (2005); Liu (2006, 2008)] and ACA [Kolk, Weber and Kuhn (2005); Kolk and Kuhn (2006); Benedetti, Aliabadi and Davì (2008); Benedetti, Milazzo and Aliabadi (2009); Weber, Kolk and Kuhn (2009)] have been well documented. In the field of fast BEM in elastodynamics, one can conduct Chen, Chew and Zeroug (1997), Fujiwara (1998, 2000), Chaillat, Bonnet and Semblat (2008), Sanz, Bonnet and Dominguez (2008), Takahashi (2012) with the FMM-BEM in frequency domain, Takahashi, Nishimura and Kobayashi (2003) with the FMM-BEM in time domain, Wei, Wang, Wang and Huang (2012) with FMM- dual reciprocity BEM, Benedetti and Aliabadi (2010) with the ACA-BEM in frequency domain and Messner and Schanz (2010) with the ACA-BEM in conjunction with CQM in time domain.

One can notice that the kernel functions of the classic time domain BEM for three-dimensional elastodynamics are monotonically decreasing with the distance $r$ between source and field points. This feature is similar to that for elastostatics and hence enables the ACA to be employed directly to compress the coefficient matrices at each time step when a direct time stepping scheme is used. In this paper, the use of ACA-accelerated time domain BEM based on direct time stepping is presented for three-dimensional dynamic analyses of the HTR-PM nuclear island foundation. At each time step, the BEM matrices based on integrations of the time domain kernel functions are approximated by using the ACA with reasonably reduced memory requirements. The following BEM matrix-vector multiplications in solving the equation system are then approximated by ACA matrix-vector multiplications with reduced operations. For discretization of the BIE, the collocation method and the eight-node discontinuous quadratic element are employed. In order to preserve the causality condition an element subdivision technique suggested by Marrero (2003) is adopted and the corresponding element integration strategy is introduced. In the numerical tests, a stability analysis is carried out in order to determine suitable time step size firstly. Then the efficiency of the ACA in terms of compression ratios of the BEM matrices at each time step is studied, followed by a sensitivity analysis on the effective compliances of the HTR-PM nuclear island foundation in terms of load frequency and soil properties by using ACA-accelerated time domain BEM. Based on this, a fixed base criterion of the soil medium for the HTR-PM nuclear island foundation is suggested for the following seismic design of nuclear structures.

## 2 Time domain BEM for 3-D elastodynamics using direct time stepping

In this section, basic formula of the time domain BEM for three-dimensional elastodynamics using direct time stepping is briefly reviewed. By assuming initial conditions and body forces to be zero, the time domain BIE governing elastodynamics in a three-dimensional homogenous domain is expressed as,

$$\begin{aligned} &c_{ij}(x)\,u_j(x,t)+\int_0^t\int_S T_{ij}^*(x,t;y,\tau)\,u_j(y,\tau)\,dS(y)d\tau \\ &=\int_0^t\int_S G_{ij}^*(x,t;y,\tau)\,t_j(y,\tau)\,dS(y)d\tau \end{aligned} \tag{1}$$

where $x$ and $y$ denote the source and field points at the boundary $S$, respectively; $u_i$ and $t_i$ are the boundary displacement and traction respectively; $c(x)$ is 0.5 for smooth boundaries; $G_{ij}^*$ and $T_{ij}^*$ are the displacement and traction kernel functions for three-dimensional elastodynamics respectively [Manolis and Beskos (1988)],

$$\begin{aligned} &G_{ij}^*(x,t;y,\tau)\overset{t'=t-\tau}{=} \\ &\frac{1}{4\pi\rho}\left[a_{ij}(r)\,\delta\left(t'-\frac{r}{c_1}\right)+b_{ij}(r)\,\delta\left(t'-\frac{r}{c_2}\right)+c_{ij}(r)\int_{1/c_1}^{1/c_2}\delta\left(t'-\lambda r\right)\lambda d\lambda\right] \end{aligned} \tag{2}$$

$$\begin{aligned} &T_{ij}^*(x,t;y,\tau)\overset{t'=t-\tau}{=} \\ &=\frac{1}{4\pi}\left[d_{ij}(r)\,\delta\left(t'-\frac{r}{c_1}\right)+e_{ij}(r)\,\delta\left(t'-\frac{r}{c_2}\right)+f_{ij}(r)\int_{1/c_1}^{1/c_2}\delta\left(t'-\lambda r\right)\lambda d\lambda\right. \\ &\left.+\,g_{ij}(r)\,\dot{\delta}\left(t'-\frac{r}{c_1}\right)+h_{ij}(r)\,\dot{\delta}\left(t'-\frac{r}{c_2}\right)\right] \end{aligned} \tag{3}$$

with $r$ being the distance between $x$ and $y$. $\rho$ is density. $c_1$ and $c_2$ are velocities of compression and shear waves (P and S waves) defined as,

$$c_1=\sqrt{\frac{2-2v}{1-2v}\frac{G}{\rho}},\quad c_2=\sqrt{\frac{G}{\rho}} \tag{4}$$

with $G$ and $v$ being the shear modulus and Poisson's ratio, respectively. The coefficients $a_{ij}$, $b_{ij}$, $c_{ij}$, $d_{ij}$, $e_{ij}$, $f_{ij}$, $g_{ij}$ and $h_{ij}$ in Eqs. (2) and (3) are functions of $r$ given by Manolis and Beskos (1988).

In order to discretize the time domain of Eq. (1), a direct time stepping scheme is used with the time axis divided into $N$ equal steps inside which the boundary variables $u_i$ are assumed to vary piecewise linearly and $t_i$ are assumed piecewise constant,

$$
\begin{aligned}
u_i(x,t) &= \sum_{n=1}^{N} \left[ \frac{t_n - t}{\Delta t} u_i^{n-1}(x) + \frac{t - t_{n-1}}{\Delta t} u_i^n(x) \right] \phi_n(t) \\
t_i(x,t) &= \sum_{n=1}^{N} t_i^n(x) \phi_n(t)
\end{aligned}
\tag{5}
$$

where $u_i^n$ and $t_i^n$ are the displacement and traction at the $n$-th time step denoted by $t_n$, $\Delta t$ is the time step size, $\phi_n(t)$ is the time interpolation function. By using Eq. (5) one can obtain time domain integrals analytically and hence Eq. (1) is rewritten as,

$$
\begin{aligned}
& c_{ij}(x) u_j^N(x) + \int_S T_{ij}^{1,0}(x,y) u_j^N(y)\, dS - \int_S G_{ij}^0(x,y) t_j^N(y)\, dS = \\
& \sum_{n=1}^{N-1} \int_S G_{ij}^n(x,y) t_j^{N-n}(y)\, dS - \sum_{n=1}^{N-1} \int_S \left[ T_{ij}^{1,n}(x,y) + T_{ij}^{2,n}(x,y) \right] u_j^{N-n}(y)\, dS
\end{aligned}
\tag{6}
$$

where $G_{ij}^n(x,y)$ is temporal integral of $G_{ij}^*$ at the $n$-th time step, $T_{ij}^{1,n}(x,y)$ and $T_{ij}^{2,n}(x,y)$ are temporal integrals of $T_{ij}^*$ at the $n$-th time step due to linear variation of $u_i$. Detailed expressions of $G_{ij}^n(x,y)$, $T_{ij}^{1,n}(x,y)$ and $T_{ij}^{2,n}(x,y)$ are referred to Manolis and Beskos (1988).

In order to discretize the space domain, we use collocation method and eight-node quadratic element. To treat the strongly-singular integrals arising from $T_{ij}^{1,n}(x,y)$ and $T_{ij}^{2,n}(x,y)$, the concept of finite part integral is used. In order to satisfy continuity requirements of the finite part integral and to treat the corner problem in a generalized manner, we adopt discontinuous elements from Mi and Aliabadi (1992) as shown in Fig. 1, where the positioning parameter $0 < \lambda < 1$ of collocation nodes stands for the degree of continuity.

In the case of the wave front traveling across a boundary element, the causality condition needs to be preserved in order that part of this boundary element keeps "quiet" before the wave front arrives. To achieve this we adopt an element subdivision technique suggested by Marrero (2003). As shown in Fig. 2, an element is divided into $m \times m$ uniform sub-elements at the local coordinate space. If a sub-element partially or entirely falls into the range of $nc_2\Delta t < r < (n+1)c_1\Delta t$, the integrations within this sub-element are calculated; otherwise the integrations are zero.

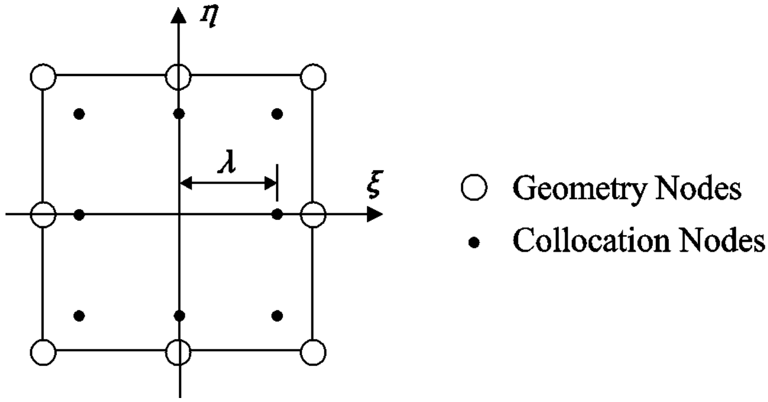


Figure 1: Eight-node discontinuous element

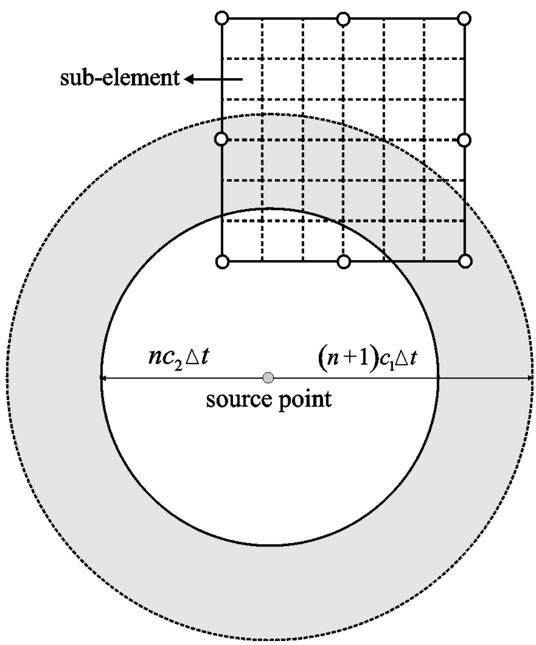


Figure 2: Element subdivision technique

Based on this approach, an element integration strategy on space domain is introduced. For each element we find a smallest sphere with radius $R_E$ enclosing the entire element. The distance between center of the sphere and the source point is denoted by $R_0$. At each time step:

1. If Eq. (7) is satisfied, the integrations on this element are zero.
2. If Eq. (8) is satisfied, the integrations on this element are calculated in the conventional manner.
3. Otherwise, the subdivision technique applied to this element.

$$\frac{R_0 - R_E}{c_1} > (n+1)\Delta t, \quad \text{or} \quad \frac{R_0 + R_E}{c_2} < n\Delta t \tag{7}$$

$$\begin{cases} \left[\frac{R_0-R_E}{c_1} > n\Delta t, \frac{R_0-R_E}{c_2} > (n+1)\Delta t, \frac{R_0+R_E}{c_1} < (n+1)\Delta t\right], \text{ or} \\ \left[\frac{R_0-R_E}{c_1} > n\Delta t, \frac{R_0+R_E}{c_2} < (n+1)\Delta t\right], \text{ or} \\ \left[\frac{R_0+R_E}{c_1} < n\Delta t, \frac{R_0-R_E}{c_2} > (n+1)\Delta t\right], \text{ or} \\ \left[\frac{R_0+R_E}{c_1} < n\Delta t, \frac{R_0-R_E}{c_2} > n\Delta t, \frac{R_0+R_E}{c_2} < (n+1)\Delta t\right] \end{cases} \tag{8}$$

After discretization on both time and space domains, one obtains a compact matrix form,

$$[c]\left\{u^N\right\} + \left[T^{1,0}\right]\left\{u^N\right\} - \left[G^0\right]\left\{t^N\right\} = \sum_{n=1}^{N-1}\left[G^n\right]\left\{t^{N-n}\right\} - \sum_{n=1}^{N-1}\left[T^{1,n} + T^{2,n}\right]\left\{u^{N-n}\right\} \tag{9}$$

## 3 ACA-accelerated Time domain BEM

In this section, basic idea of the ACA and procedures of ACA-accelerated time domain BEM are summarized. The ACA is an algebraic approximation algorithm which is based only on the knowledge of the matrix entries. This kernel-independent feature makes it easy to apply the ACA directly for the solution of various BEM problems. The basic idea of ACA is that a low-rank matrix denoted by $[A]_{m\times n}$ can be approximated by a sum of vector-vector multiplications,

$$[A]_{m\times n} \approx \sum_{i=1}^{k}\left\{U^i\right\}\left\{V^i\right\}^T = [U]_{m\times k}[V]_{k\times n} \tag{10}$$

As $k \ll m,n$, both the memory requirement of $[A]_{m\times n}$ and the following operations of the maitrx-vector multiplication is reduced from $O(m\times n)$ to $O(k\times(m+n))$.

Basically there are two types of ACA, namely the fully-pivoted and partially-pivoted ACA [Bebendorf (2003)]. The former algorithm requires the knowledge of all matrix entries with $O(m \times n)$ operations before preforming ACA approximation; the latter one requires the knowledge of only a small amount of matrix entries, therefore regarded as a truly fast version. However for vector problems like the three-dimensional elastodynamics, it is more convenient to calculate a set of entries related to one element rather than obtaining a single entry. Therefore in this paper the fully-pivoted ACA is employed, which is described as the following scheme: First find a largest absolute value of $[A]_{m\times n}$ in the row $i_1$ and column $j_1$. The first pair of vectors $\left\{U^1\right\}$ and $\left\{V^1\right\}$ are defined as,

$$\begin{aligned} U_i^1 &= A_{i,j_1}, \quad i = 1..m \\ V_j^1 &= \frac{A_{i_1,j}}{A_{i_1,j_1}}, \quad j = 1..n \end{aligned} \tag{11}$$

The first residual matrix is calculated as,

$$\left[R^1\right]_{m\times n} = [A]_{m\times n} - \left\{U^1\right\}\left\{V^1\right\}^T \tag{12}$$

Then the operation is restarted for $\left[R^1\right]_{m\times n}$ and new vectors $\left\{U^2\right\}, \left\{V^2\right\}$ and residual matrix $\left[R^2\right]_{m\times n}$ are obtained. By recursively performing this operation, one obtaines,

$$\left[R^k\right]_{m\times n} = \left[R^{k-1}\right]_{m\times n} - \left\{U^k\right\}\left\{V^k\right\}^T \tag{13}$$

The operation stops when $\left\|\left[R^k\right]_{m\times n}\right\|_F$ is smaller than a prescribed residual error and then $\left[R^k\right]_{m\times n}$ can be neglected. Based on the ACA approximation of one low-rank matrix, procedures of the ACA-accelerated time domain BEM is described as follows,

***Step 1:***

An adaptive tree is constructed according to the geometry information of the boundary elements. First, A cubic root is established enclosing the entire boundary element model; the root is then divided into sub-cubes of equal size, so called "tree nodes", each containing a set of boundary elements; this division is performed recursively until the number of boundary elements contained in a tree node is less than a prescribed number of $m$. Within this paper we use $m$ = 1 as one element contains 24 number of freedoms.

***Step 2:***

At each time step of the time domain BEM, the coefficient matrices $[G^n]$ and $\left[T^{1,n}\right]$, $\left[T^{2,n}\right]$ of Eq. (9) are partitioned into sub-matrices respectively at various levels. Each sub-matrix arises from the interaction of two sets of boundary elements belonging to specific tree nodes.

***Step 3:***

Identify the low-rank sub-matrices according to the size and distance information of the associated tree nodes. After identification, the full-rank matrices are calculated directly in a conventional manner; the low-rank matrices are calculated firstly and then approximated with a sum of vector-vector multiplications by using the ACA.

***Step 4:***

The coefficient matrix-vector multiplications in Eq. (9) are approximated by a sum of direct sub-matrix-vector multiplications and ACA sub-matrix-vector multiplications.

## 4 Numerical results

A C++-based BEM code has been developed for the ACA-accelerated time domain BEM for three-dimensional elastodynamic analysis. In the code, each entry is calculated and stored as an *eight-byte* value. In order to assess validity of the presented method, a number of numerical tests have been carried out, including a stability analysis on the time step size and a sensitivity study on the dynamic responses of the HTR-PM nuclear island foundation in terms of both the load frequency and supporting soil properties. The code runs on a desktop computer with a processor of Intel Xeon CPU E31245 and physical memory of 8GB.

In the following, the relative error of convergence in GMRES is taken to be $10^{-5}$; the error for stop in the fully-pivoted ACA is taken to be $10^{-5}$

### *4.1 Stability analysis on the time step size*

This test involves dynamic analysis of a $2 \times 2 \times 4$ elastic rod fixed at one end and subjected to a constant unit pressure at the opposite free end at $t = 0$. The rest boundaries are free. The Young's modulus and Poisson's ratio is 2000.0 and 0.0 respectively; the density is 1000.0; the element degree of continuity $\lambda$ is taken to be 2/3. In order to study the effect of the time step size $\Delta t$ on stability of the time domain BEM, we adopt a widely used dimensionless parameter to represent $\Delta t$,

$$\beta = \frac{c_1 \Delta t}{L_e} \tag{14}$$

where $L_e$ is the representative element edge size. The rod surface is discretized into 40 discontinuous elements with element edge size taken to be 1.0. The total number of degree of freedoms (DOF) is 960. We select $\beta$ to be 0.2, 0.4, 0.6 and 0.8 for the stability analysis, and the number of total time steps in the calculation is taken to be 300. The longitudinal displacement at the loaded end of the rod is outputted versus time. Significant instability of the displacement is observed for $\beta = 0.2, 0.6, 0.8$. Only the case of $\beta = 0.4$ results in good displacement stabilities along all time steps as shown in Fig. 3 in comparison with analytical results. Therefore, $\beta = 0.4$ is determined for the following analyses.

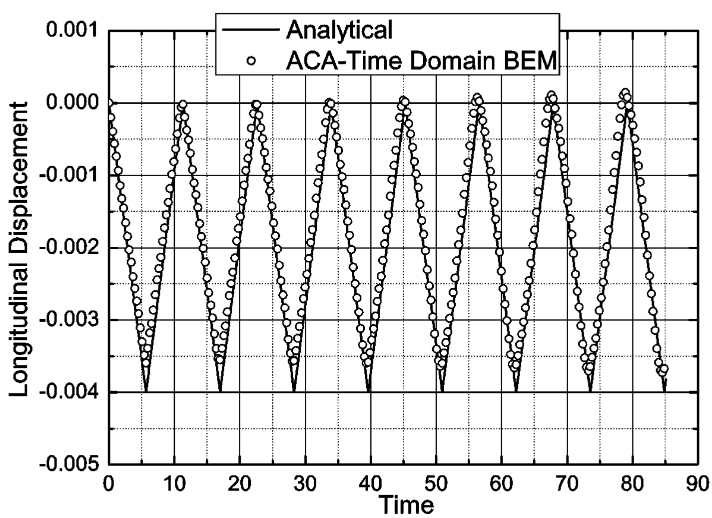


Figure 3: Longitudinal displacement at loaded end of the rod ($\beta = 0.4$)

### 4.2 Dynamic analyses of HTR-PM nuclear island foundation

This test involves a study on compression efficiency of the ACA when treating coefficient matrices of the time domain BEM, followed by a sensitivity analysis on dynamic characteristics of the HTR-PM nuclear island foundation in terms of load frequency and soil properties.

The investigated domain is a HTR-PM nuclear island foundation located on the surface of a homogenous half-space soil medium. This irregular foundation supports three nuclear grade buildings, namely the reactor building, the spent fuel storage building and the auxiliary building. Fig. 4 shows geometrical information of the foundation with surrounding finite soil surface to be studied. For convenience the foundation is assumed to be rigid. It is subjected to a translational harmonic displacement load with amplitude of $\bar{U} = 0.1$m at horizontal-X (HOR-X) or vertical direction as defined in Fig. 4. It is fixed on the other orthogonal directions. A modified compliance of the foundation is defined herein in order to represent dynamic characteristics of the foundation and to help establish a fixed base criterion,

$$C_m = \frac{\bar{U}}{T_f} \tag{15}$$

where $T_f$ is the amplitude of the total reaction force on the foundation.

As variables to be used in the sensitivity analysis, values of the load frequency (denoted by $f$) and soil properties listed in Tables 1 and 2 are considered. The frequency ranges from 1.0 to 25.0 Hz, covering most interested frequencies of the design basis earthquake in the seismic design of of a NPP. The shear wave velocities of the soil medium ranges from 700 to 2000 m/s, covering typical values of the soil profiles at most Chinese NPP sites.

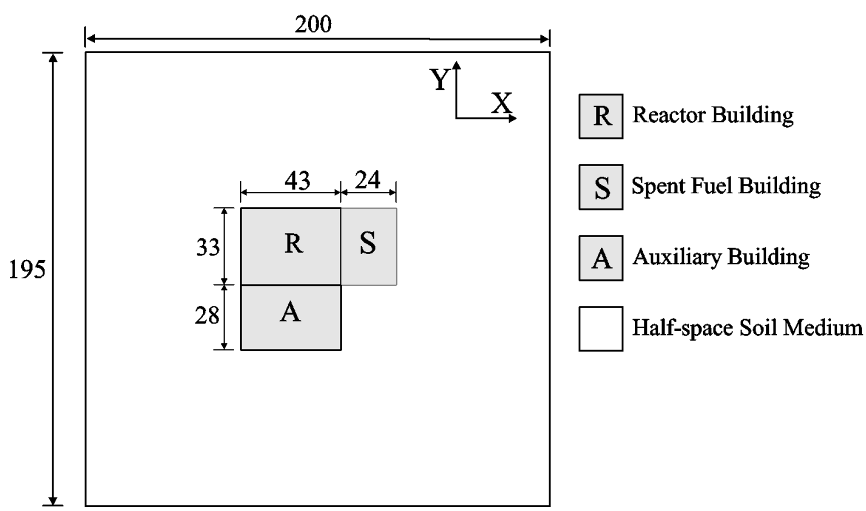


Figure 4: Sizes of the investigated domain containing HTR-PM nuclear island foundation and surrounding soil surface (unit: m)

Table 1: Values of the load frequency

| No. | 1 | 2 | 3 | 4 | 5 | 6 | 7 |
|---|---|---|---|---|---|---|---|
| $f$ (Hz) | 1.0 | 3.0 | 5.0 | 8.0 | 12.0 | 18.0 | 25.0 |

Table 2: Values of soil properties

| No. | $c_2$ (m/s) | $\rho$ (kg/m3) | $\nu$ |
|---|---|---|---|
| 1 | 700 | 2150 | 0.34 |
| 2 | 1100 | 2500 | 0.32 |
| 3 | 1500 | 2500 | 0.32 |
| 4 | 2000 | 2750 | 0.26 |

First, compressions of the coefficient matrices $[G^n]$ and $[T^{1,n}]$ in Eq. (9) by using ACA are tested. The domain is discretized with 72, 306 and 576 boundary elements respectively, with DOFs to be 1728, 7344 and 13824 respectively. Fig. 5 shows 306 boundary elements (each element is plotted as four corner collocation nodes connected with solid lines in order only to show the effect of discontinuity). The No. 1 of soil properties listed in Table. 2 is used. The accumulative memory requirements of compressed $[G^n]$ and $[T^{1,n}]$ by using ACA along time steps are plotted in Figs. 6 and 7 respectively in comparison with that of full-rank matrices. Herein the memory is normalized with storage of one full-rank matrix as unit.

It is shown that the compression ratio decreases slowly with increasing boundary element scales. At DOF = 13824, the final compression ratio is less than 32%. It should be pointed out that this compression ratio attributes not only to the ACA, but also to the nature of sparse matrices at beginning and end of time steps. However, this sparse feature is easily identified and utilized by the ACA as zero sub-matrices are automatically neglected. It is also observed that the compression ratio is almost the same for $[G^n]$ and $[T^{1,n}]$

Next, modified compliance $C_m$ of the HTR-PM nuclear island foundation at HOR-X and vertical directions are calculated in terms of the load frequency and soil properties listed in Tables 1 and 2. Discretization of the domain with quadratic boundary elements is determined with an element size criterion given by,

$$L_e \leq \frac{1}{2}\frac{c_2}{f} \tag{16}$$

Fig. 8 shows calculated reaction force of the foundation at HOR-X direction with $f$ = 5.0 and 12.0 Hz and soil properties of No. 2 in Table. 2. It is shown that for

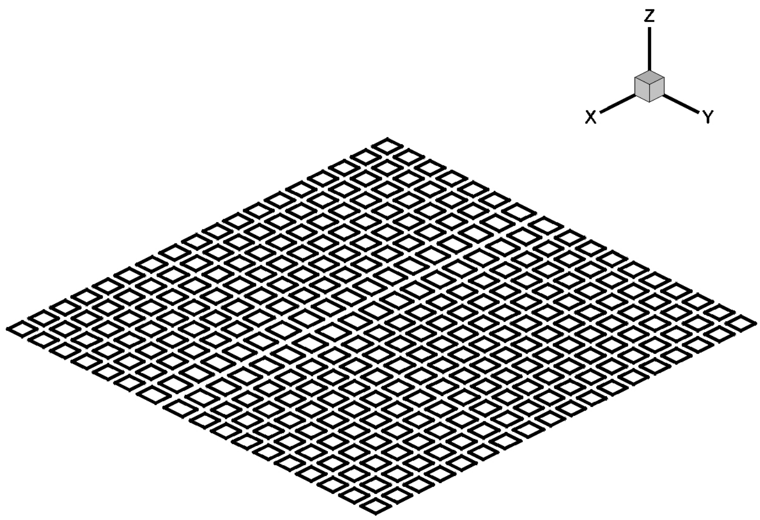


Figure 5: Boundary elements of the foundation and surrounding soil surface

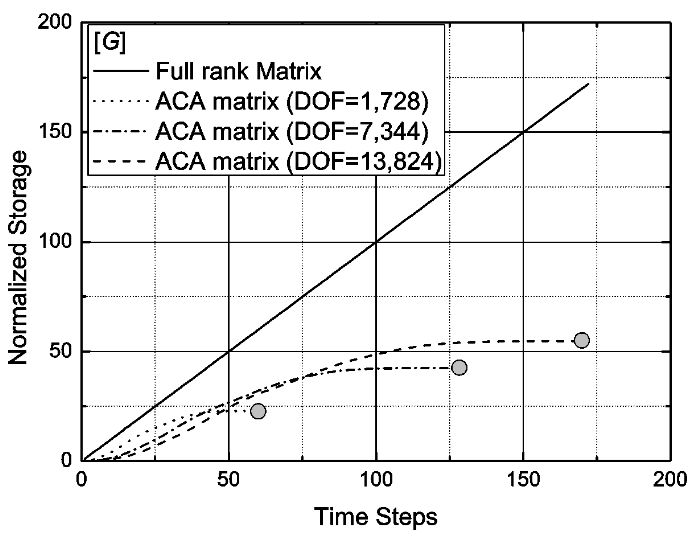


Figure 6: Storage of ACA-Compressed $[G^n]$

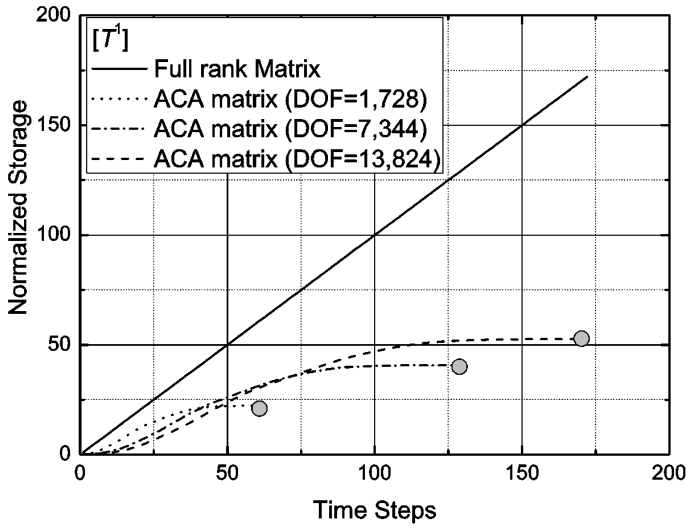


Figure 7: Storage of ACA-Compressed $\left[T^{1,n}\right]$

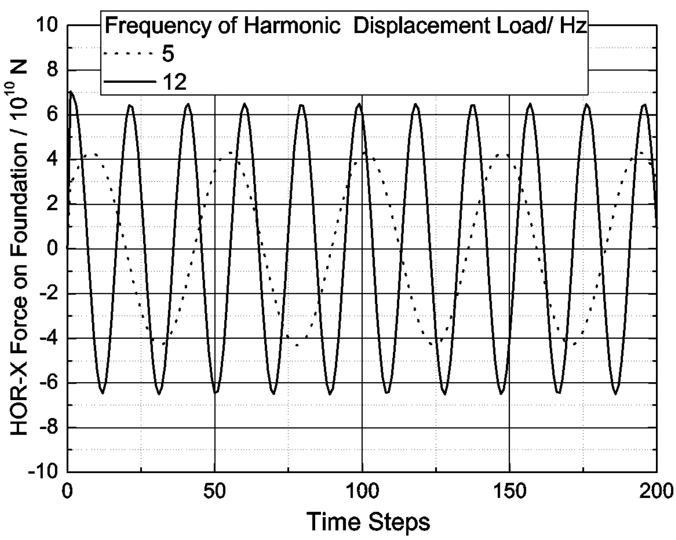


Figure 8: Horizontal reaction force of the foundation at $f$ = 5.0 and 12.0 Hz

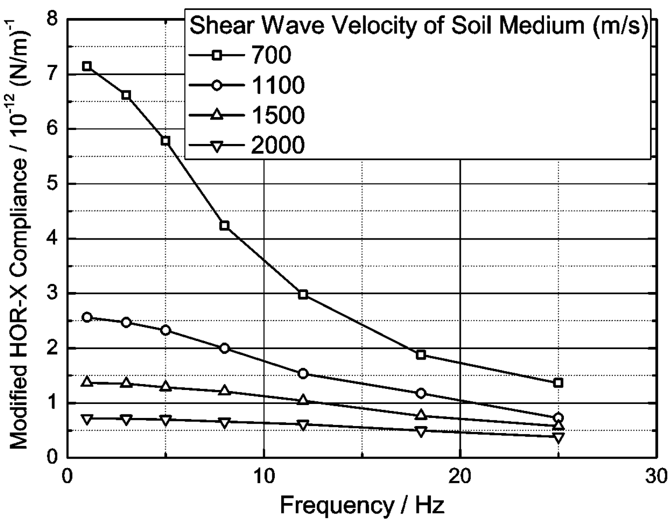


Figure 9: $C_m$ at HOR-X direction

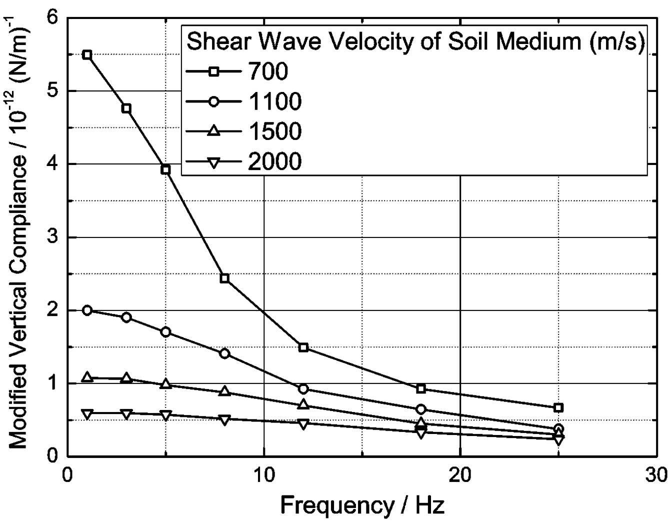


Figure 10: $C_m$ at vertical direction

this problem the time domain BEM has good stabilities. Figs. 9 and 10 show the calculated $C_m$ in terms of load frequency and soil properties. It is clearly shown that $C_m$ decreases with increasing shear wave velocities. In the case of $c_2$ = 700 m/s, $C_m$ varies with load frequency significantly at nearly one order of magnitude; when $c_2$ = 2000 m/s, $C_m$ remains nearly unchanged compared with that of lower values of $c_2$ Fig. 11 shows the vertical displacement at the 26-th time step with DOF = 7344, $f$ = 25.0 Hz and soil properties of No. 2 in Table. 2. Clear wave propagations are observed.

The above observations indicate that the soil medium with $c_2$ = 2000 m/s is rigid enough at all interested frequencies that it can be assumed as a fixed base for the HTR-PM nuclear island foundation. Therefore, it is recommended that shear wave velocity of 2000 m/s at foundation level be a fixed base criterion for site selection and seismic design of the HTR-PM nuclear power plants.

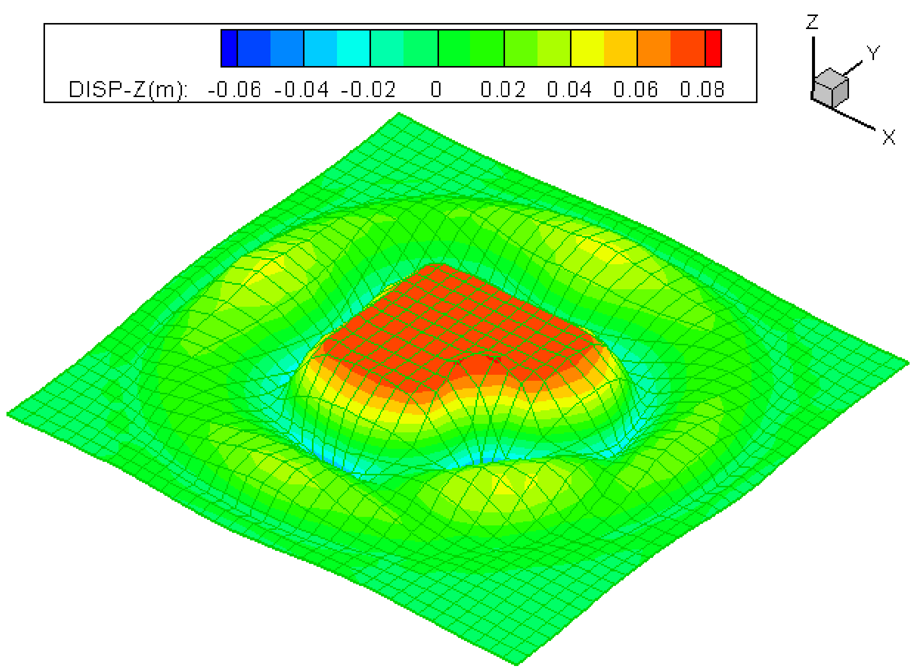


Figure 11: Vertical displacement at the 26-th time step (DOF = 7344, $f$ = 25.0 Hz, No.2 soil properties)

## 5 Conclusions

The use of ACA-accelerated time domain BEM based on direct time stepping scheme has been presented for three-dimensional dynamic analyses of the HTR-PM nuclear island foundation. At each time step, the BEM matrices were compressed by using the ACA with memory requirements reasonably decreased. The BEM matrix-vector multiplications were then replaced with ACA matrix-vector operations. In order to discretize the BIE on the space domain the collocation method and the eight-node discontinuous quadratic element were employed. The causality condition was guaranteed by employing an element subdivision technique. Based on this, an element integration strategy is introduced.

In the numerical examples, the proposed method was firstly tested in a stability analysis in order to determine suitable time step size. The value of $\beta = 0.4$ was observed to result in good stabilities. Then the efficiency of the ACA in terms of accumulative storage of BEM matrices along the time steps was studied. It was observed that larger BEM scales result in better compression ratio of the BEM matrices by using the ACA. Finally, a sensitivity analysis on dynamic characteristics of the HTR-PM nuclear island foundation in terms of load frequency and soil properties by using ACA-accelerated time domain BEM was carried out. It was observed that higher shear wave velocities result in lower and more stable compliances. Based on this, a fixed base criterion of the soil medium for the HTR-PM nuclear island foundation was recommended.

## Acknowledgement

Financial supports for the project from the National Natural Science Foundation of China, under grant No. 11072128 and No. 11002080 are gratefully acknowledged.

## References

**Antes, H.** (1985): A boundary element procedure for transient wave propagations in two-dimensional isotropic elastic media. *Finite Elements in Analysis and Design*, vol. 1, pp. 313–322.

**Bebendorf, M.; Rjasanow, S.** (2003): Adaptive low-rank approximation of collocation matrices. *Computing*, vol. 70, pp. 1–24.

**Benedetti, I.; Aliabadi, M. H.; Davì, G.** (2008): A fast 3D dual boundary element method based on hierarchical matrices. *Int J Solids and Structures*, vol. 45, pp. 2355–2376.

**Benedetti, I.; Milazzo, A.; Aliabadi, M. H.** (2009): A fast dual boundary element method for 3D anisotropic crack problems. *Int J Numer Methods Engng* vol. 80, pp. 1356–1378.

**Benedetti, I.; Aliabadi, M. H.** (2010): A fast hierarchical dual boundary element method for three-dimensional elastodynamic crack problems. *Int J Numer Methods Engng*, vol. 84, pp. 1038–1067.

**Beskos, D. E.** (1987): Boundary element methods in dynamic analysis. *Applied Mechanics Review*, vol. 40, no. 1, pp. 1–23.

**Beskos, D. E.** (1997): Boundary element methods in dynamic analysis: PartII (1986–1996). *Applied Mechanics Review*, vol. 50, no. 3, pp. 149–197.

**Birgisson, B.; Siebrits, E.; Peirce, A. P.** (1999): Elastodynamic direct boundary element methods with enhanced numerical stability properties. *Int J Numer Methods Engng*, vol. 46, pp. 871–888.

**Chaillat, S.; Bonnet, M.; Semblat, J. F.** (2008): A multi-level fast multipole BEM for 3-D elastodynamics in the frequency domain. *Computer Methods in Applied Mechanics and Engineering*, vol. 197, no. 49–50, pp. 4233–4249.

**Chen, Y. H.; Chew, W. C.; Zeroug, S.** (1997): Fast multiple method as an efficient solver for 2D elastic wave surface integral equations. *Comp Mech*, vol. 20, pp. 495–506.

**Cruse, T. A.; Rizzo, F. J.** (1968): A direct formulation and numerical solution of the general transient elastodynamic problemI. *Journal of Mathematical Analysis and Applications*, vol. 22, pp. 244–259.

**Dominguez, J.** (1993): *Boundary elements in dynamics.* Southampton, Boston, Computational Mechanics Publications.

**Fu, Y. H.; Klimkowski, K. J.; Rodin, G. J.; Berger, E.; Browne, J. C.; Singer, J. K.; Geijn, R. A.; Vernaganti, K. S.** (1998): A fast solution method for three-dimensional many-particle problems of linear elasticity. *Int J Numer Methods Engng*, vol. 42, pp. 1215–1229.

**Fujiwara, H.** (1998): The fast multipole method for integral equations of seismic scattering problems. *Geophys J Int*, vol. 133, pp. 773–782.

**Fujiwara, H.** (2000): The fast multiple method for solving integral equations of three-dimensional topography and basin problems. *Geophys J Int*, vol. 140, pp. 198–210.

**Gaul, L.; Schanz, M.** (1999): A comparative study of three boundary element approaches to calculate the transient response of viscoelastic solids with unbounded domains. *Comput Methods Appl Mech Engrg*, vol. 179, pp. 111–123.

**Greengard, L.; Rokhlin, V.** (1997): A fast algorithm for particle simulations. *J Comput Phys*, vol. 135, pp. 280–292.

**Greengard, L.; Rokhlin, V.** (1997): A new version of the fast multipole method for the Laplace equation in three dimensions. *Acta Numer*, vol. 6, pp. 229–270.

**Helsing, J.** (1999): Fast and accurate numerical solution to an elastostatic problem involving ten thousand randomly oriented cracks. *Int J Fracture*, vol. 100, no. 4, pp. 321–327.

**Kielhorn, L.; Schanz, M.** (2008): Convolution quadrature method-based symmetric Galerkin boundary element method for 3-d elastodynamics. *Int J Numer Methods Engng*, vol. 76, pp. 1724–1746.

**Kolk, K.; Weber, W.; Kuhn, G.** (2005): Investigation of 3D crack propagation problems via fast BEM formulations. *Comput Mech* vol. 37, pp. 32–40.

**Kolk, K.; Kuhn, G.** (2006): The advanced simulation of fatigue crack growth in complex 3D structures. *Archive of Applied Mechanics*, vol. 76, no. 11-12, 699–709.

**Liu, Y. J.; Nishimura, N.; Otani, Y.; Takahashi, T.; Chen, X. L.; Munakata, H.** (2005): A fast boundary element method for the analysis of fiber-reinforced composites based on a rigid-inclusion model. *J Appl Mech*, vol. 72, no. 1, pp. 115–128.

**Liu, Y. J.** (2006): A new fast multipole boundary element method for solving large-scale two-dimensional elastostatic problems. *Int J Numer Methods Engng*, vol. 65, no. 6, pp. 863–881.

**Liu, Y. J.** (2008): A fast multipole boundary element method for 2D multi-domain elastostatic problems based on a dual BIE formulation, *Comp Mech* vol. 42, no. 5, pp. 761–773.

**Lubich, C.** (1988): Convolution quadrature and discretized operational calculus I, *Numerische Mathematik*, vol. 52, pp. 129–145.

**Lubich, C.** (1988): Convolution quadrature and discretized operational calculus II, *Numerische Mathematik*, vol. 52, pp. 413–425.

**Lubich, C.** (2004): Convolution quadrature revisited. *BIT Num Math*, vol. 44, no. 3, pp. 503–514.

**Manolis, G. D.; Beskos, D. E.** (1988): Boundary element methods in elastodynamics. *London : Unwin Hyman*

**Mansur, W. J.** (1983): A time-stepping technique to solve wave propagation problems using the boundary element method. *Ph.D. Thesis*, *University of Southampton*.

**Mansur, W. J.; Carrer, J. A. M.; Siqueira, E. F. N.** (1998): Time discontinuous linear traction approximation in time-domain BEM scalar wave propagation. *Int J Numer Methods Engng*, vol. 42, no. 4, pp. 667–683.

**Messner, M.; Schanz, M.** (2010): An accelerated symmetric time-domain boundary element formulation for elasticity. *Engrg Anal Boundary Elements* vol. 34, pp. 944–955.

**Mi, Y.; Aliabadi, M. H.** (1992): Dual boundary element method for three-dimensional fracture mechanics analysis. *Engrg Anal Boundary Elements*, vol. 10, pp. 161–171.

**Peirce, A.; Siebrits, E.** (1997): Stability analysis and design of time-stepping schemes for general elastodynamic boundary element models. *Int J Numer Methods Engng*, vol. 40, no. 2, pp. 319–342.

**Popov, V.; Power, H.** (2001): An O(N) Taylor series multipole boundary element method for three-dimensional elasticity problems. *Engrg Anal Boundary Elements*, vol. 25, pp. 7–18.

**Rizos, D. C.; Karabalis, D. L.** (1994): An advanced direct time domain BEM formulation for general 3-D elastodynamic problems. *Comput Mech*, vol. 15, pp. 249–269.

**Rokhlin, V.** (1985): Rapid solution of integral equations of classical potential theory. *J Comput Phys*, vol. 60, pp. 187–207.

**Sanz, J. A.; Bonnet, M.; Dominguez, J.** (2008): Fast multipole method applied to 3-D frequency domain elastodynamics. *Engrg Anal Boundary Elements*, vol. 32, pp. 787–795.

**Schanz, M.; Antes, H.** (1997): A new visco- and elastodynamic time domain boundary element formulation, *Comput Mech*, vol. 20, no. 5, pp. 452–459.

**Schanz, M.** (2001): Application of 3D time domain boundary element formulation to wave propagation in poroelastic solids. *Engrg Anal Boundary Elements*, vol. 25, pp. 363–376.

**Takahashi, T.; Nishimura, N.; Kobayashi, S.** (2003): A fast BIEM for three-dimensional elastodynamics in time domain. *Engrg Anal Boundary Elements*, vol. 27, pp. 491–506.

**Takahashi, T.** (2012): A wideband fast multipole accelerated boundary integral equation method for time-harmonic elastodynamics in two dimensions. *Int J Numer Meth Engng*, vol. 91, pp. 531–551.

**Tsinopoulos, S. V.; Polyzos, D.; Beskos, D. E.** (2012): Static and Dynamic BEM Analysis of Strain Gradient Elastic Solids and Structures. *CMES: Computer Modeling in Engineering & Science* vol. 86, no. 2, pp. 113–144.

**Wang, H. T.; Yao, Z. H.** (2005): A new fast multipole boundary element method for large scale analysis of mechanical properties in 3-D particle-reinforced composites. *CMES: Computer Modeling in Engineering & Science*, vol. 7, no. 1, pp. 85–95.

**Weber, W.; Kolk, K.; Kuhn, G.** (2009): Acceleration of 3D crack propagation simulation by the utilization of fast BEM-techniques. *Engrg Anal Boundary Elements* vol. 33, no. 8-9, pp. 1005–1015.

**Wei, Y.; Wang, Q.; Wang, Y.; Huang, Y.** (2012): Optimizations for Elastodynamic Simulation Analysis with FMM-DRBEM and CUDA. *CMES: Computer Modeling in Engineering & Science* vol. 86, no. 3, pp. 241–273.

**Yoshida, K.; Nishimura, N.; Kobayashi, S.** (2001): Application of fast multipole Galerkin boundary integral equation method to elastostatic crack problems in 3D. *Int J Numer Methods Engng* vol. 50, pp. 525–547.

**Yu, G.; Mansur, W. J.; Carrer, J. A. M.; Gong, L.** (1998): Time weighting in time domain BEM. *Engrg Anal Boundary Elements*, vol. 22, no. 3, pp. 175–181.

**Zhang, Z. Y.; Wu, Z. X.; Sun, Y. L.; Li, F.** (2006): Design aspects of the Chinese modular high-temperaturegas-cooled reactor HTR-PM. *Nuclear Engineering and Design*, vol. 236, pp. 485–490.